Research Article

Yifeng Ling, Peng Zhang*, Juan Wang, Peter Taylor, and Shaowei Hu

Effects of nanoparticles on engineering performance of cementitious composites reinforced with PVA fibers

https://doi.org/10.1515/ntrev-2020-0038
received March 31, 2020; accepted April 07, 2020

Abstract: In this study, the influence of nano-$CaCO_3$ (NC) and nano-SiO_2 (NS) on engineering properties of cementitious composites reinforced with polyvinyl alcohol (PVA) fibers was investigated including slump and fracture properties as well as compressive, flexural, tensile, and strengths. The influence mechanism of NS content on properties of cementitious composites was revealed. The combined effects of NS and NC were evaluated on the composites made with 0.9% volumetric PVA fiber addition. The experimental results showed that the addition of nanoparticles decreased the workability of fresh cementitious composites reinforced with PVA fibers. Higher NS content deceased more workability and NC reduced more workability than NS for the composites. There was an initial increase and later decrease in compressive and flexural strengths as NS content alters from 0% to 2.5%, while the continuous increase was found in tensile strength. 1.5% NS maximally increased compressive strength and flexural strength, while 2.5% NS is optimal for tensile strength. The composite containing NC exhibited lower strengths than the composite containing the same content of NS. The fracture energy, initiation, and unstable fracture toughness slightly increased with the NS content varying from 0% to 1.5%, while they reduced when NS content was higher than 1.5%. The effects of NS and NC on fracture energy and toughness were inapparent. The failure mode of PVA fibers in the tensile strength test was changed from pull-out to fracture with the addition of NS based on microstructure characterization.

Keywords: engineering properties, fracture properties, nano-SiO_2, nano-$CaCO_3$, microstructure, PVA fiber-reinforced composite

1 Introduction

While traditional cementitious composites have found many applications in global infrastructure, they do come with some challenges including low ductility and high fracture tendency [1,2]. As a solution, polyvinyl alcohol (PVA) fiber is usually used to reduce fracture tendency and control the propagation of cracks in cementitious composites [3]. The bending resistance and durability of cementitious composites can be improved remarkably [4,5]. PVA fiber mainly increases the toughness of the cementitious composite by reducing stress concentrations on internal defects [6]. In a study by Yu et al., the tensile stress and strain capacities of the concrete were enhanced because of the increased toughness [7]. Based on tests of dynamic tensile properties, Cadoni et al. concluded PVA fiber addition considerably enhanced tensile strain capacity and strength by reducing fracture energy [8]. A study by Haskett et al. focused on the influence of PVA fiber in stress zone of concrete and concluded that PVA fibers effectively reduced the crack number of compressive zone [9]. Even after cracks appear, composites containing PVA fibers have strain hardening performance associated with the bridge effect of the fiber in tension zone [10].

However, a large number of study results have indicated that PVA fibers were prone to be pulled out in tension because of relatively small bonding strength between the fiber and matrix. Ma et al. reported that the existence of fly ash in the cementitious composites

* **Corresponding author: Peng Zhang,** School of Water Conservancy Engineering, Zhengzhou University, Zhengzhou, 450001, China, e-mail: zhangpeng@zzu.edu.cn
Yifeng Ling: School of Civil Engineering, Hunan University of Technology, Zhuzhou, 412007, China; National Concrete Pavement Technology Center, Institute for Transportation, IA 50014, Ames, United States of America
Juan Wang: School of Water Conservancy Engineering, Zhengzhou University, Zhengzhou, 450001, China
Peter Taylor: National Concrete Pavement Technology Center, Institute for Transportation, IA 50014, Ames, United States of America
Shaowei Hu: School of Water Conservancy Engineering, Zhengzhou University, Zhengzhou, 450001, China; College of Civil Engineering, Chongqing University, Chongqing, 400045, China

reinforced with PVA fibers could weaken the bonding strength between the fiber and matrix owing to small hydration rate of fly ash [11]. Li et al. found that failures of fibers under tension were composed of pulling out with tiny wearing, superficial wearing, and an end with partial peeling [12]. The same fibers pullout also occurred in geopolymer composite containing fly ash [8]. Atahan et al. claimed that the amount of pull-out PVA fibers was high for mixtures with 0.35 w/c [13]. The previous research work indicates that with PVA fiber addition, the porosity of cement paste was increased resulting in the reduction of bond strength and the engineering properties [14,15]. Therefore, actions to reduce porosity to improve the bonding strength between the fiber and cementitious matrix is a critical need for further application of PVA fiber-reinforced composites.

On the other hand, nanoparticles have been widely used in the cementitious composite as an additive since they can significantly enhance strength and durability based on previous work. Nanoparticles were usually treated as a cementitious material in cementitious composites because of the influence on accelerating hydration and improving microstructure [16,17]. Gonzalez et al. found that the durability and strength of concretes were improved with nanoparticle inclusion [18]. The investigation of Zhang et al. indicated that 2% of content nanoparticles to cementitious composites greatly enhanced flexural and compressive strengths [19]. A 38% increase in tensile strength of the cement pastes containing 2% nanoparticles was obtained by Gesoglu et al. [20]. These improvements in engineering properties are reportedly associated with the filling effect of nanoparticles in voids and between unreacted particles in composites, which led a decrease in total porosity [21]. Additionally, the addition of nanoparticles generally improves the bonding strength of cementitious composites [22]. Among the nanoparticles, nano-$CaCO_3$ (NC) and nano-SiO_2 (NS) are mostly used nanoparticles in cementitious composites [23–26]. However, at present, there are few research results on the comparison of NC and NS particles on properties of cementitious composites including the physical properties and mechanical properties. Thereby, to understand the influence of nanoparticles on engineering properties of composites containing PVA fibers is essential to improve the bonding strength between the PVA fiber and the cementitious matrix. Related investigation on engineering properties of the composites with different types and contents of nanoparticles is very limited.

In the present study, NC and NS were adopted to enhance the engineering properties of cementitious composites reinforced with PVA fibers, including the bonding strength between the fiber and composite matrix. The effects of varied NS contents and nanoparticle types on engineering properties of cementitious composites reinforced with PVA fibers were investigated by engineering tests. A double-K fracture test was performed to determine the fracture properties of composites. Additionally, the slump and microstructure of composites were characterized.

2 Experiments

2.1 Materials

P.O42.5 Portland cement was used, which has a specific gravity (SG) of 3.13 and a specific surface (SS) of 3,266 cm^2/g [27]. According to GB/T 1596-2017 [28], the first-level fly ash with low calcium was utilized, which has SG of 2.13 and SS of 2,464 cm^2/g. Table 1 provides the properties of fly ash and cement. Short PVA fibers with the content of 0.9% were used in this study. Table 2 lists its performance indices. NC and NS were employed as nanoparticles in this investigation, the performance indices of which are presented in Table 3. The flowability

Table 1: Composition of cement and fly ash

Composition (%)	SiO_2	MgO	CaO	Al_2O_3	SO_3	Fe_2O_3	K_2O	Na_2O
Cement	21.05	3.58	63.14	5.28	2.39	2.57	0.58	0.17
Fly ash	52.12	3.26	9.12	17.86	0.23	6.57	2.05	2.38

Table 2: Performance indices of PVA fiber

SG	Tensile strength (MPa)	Melting point (°C)	Fiber diameter (μm)	Dry fracture elongation (%)	Fiber length (mm)	Water absorption (%)
1.32	1,400	220	20	15	9	<1

Table 3: Performance indices of nanoparticles

Nano particles	Content (%)	PH	SS (m^2/g)	Particle size (nm)	Bulk density (g/cm^3)
SiO_2	99.5	6	200	30	0.055
$CaCO_3$	99	9.3	23	30	0.3

Table 4: HRWR properties

SG	Reducing rate (%)	Chloride ion content (%)	PH	Alkali content (%)
1.06	22.0	0.078	4.62	1.2

of fresh composites was evaluated using a high-range water reducing admixture (HRWR), and the performance indices of HRWR can be seen in Table 4. The grain size of the fine aggregate in this study is 212–380 μm.

2.2 Mix proportions

Referring to the investigation of Yew et al., the suggested PVA fiber content used for concretes varies from 0.1% to 3.0% [29]. As a result, in this investigation, a 0.9% PVA fiber volume fraction of the mixture was used. Five different NS contents (0.0%, 1.0%, 1.5%, 2.0%, and 2.5% of binder by mass) and the fixed NC content of 2.0% were used to prepare the cementitious composites. In all, 6 proportions of cementitious composites were designed with 0.38 water to binder ratio (w/b) and 2 binders to the sand ratio (b/s) were selected. The mix proportions are shown in Table 5.

2.3 Experiment method

2.3.1 Mixture preparing

The fresh mixture of the cementitious composite was prepared using a Hobart mixer referring to the standards of ASTM C305 [30]. Due to the remarkable aggregation effect of nanoparticles, the workability of the cementitious composite was influenced greatly by the addition of NS and NC particles. To prevent the uneven dispersing of nanoparticles, different mixing methods and stirring process were tried, and the following appropriate mixing process was adopted. First, the dry cement, fly ash, nanoparticles, and silica sands were mixed for 2 min. And then, one-third water and a half HRWR were added into the mixture to be mixed for 1 min. After that, the rest HRWR and one-third of water were introduced and agitated for 1 min. Then, the rest water was poured into the mixture and mixed for 1 min. Finally, the PVA fibers were divided into 4 parts, and each part was added and mixed for 2.5 min, respectively. Before engineering performance tests, the samples should be demolded after 24 h and cured for 28 days under the standard curing condition (95% relative humidity and 20°C temperature).

2.3.2 Slump test

Since PVA fibers and nanoparticles could reduce the workability of the cementitious composite [31–33], the slump test was performed to determine the workability of studied mixtures as per ASTM C1611 Procedure A [34]. The evaluation index of slump flow was used to evaluate the workability of fresh cementitious composites. For each mixture, the average of two test results was reported.

2.3.3 Compressive strength test

For the compressive strength test, three 71 mm cube specimens were tested for each mixture according to JGJ

Table 5: Mix proportions for composites

Mixture	Cement (kg/m^3)	Fly ash (kg/m^3)	NS (kg/m^3)	NC (kg/m^3)	PVA fiber (%)	Sand (kg/m^3)	Water (kg/m^3)	HRWR (kg/m^3)
NS-0.0	650	350	0	–	0.9	500	380	3
NS-1.0	640	350	10	–	0.9	500	380	3
NS-1.5	635	350	15	–	0.9	500	380	3
NS-2.0	630	350	20	–	0.9	500	380	3
NS-2.5	625	350	25	–	0.9	500	380	3
NC-2.0	630	350	–	20	0.9	500	380	3

Note: the mixture is named using the percentage of nanoparticle contents.

70–90 [35]. The reported result was the average compressive strength of triplicates.

2.3.4 Flexural strength test

The sample used for the flexural strength experiment was 40 mm × 40 mm × 160 mm prism. For each mixture, three prisms were made. Flexural strength tests were carried out using an electric flexure tester in accordance with JTJ E30-2005 [36] as shown in Figure 1. Before the test, the specimen was put into the holder of the flexural tester, and the handwheel was turned first to make the specimen contact with the loading roller. Then, the big lever of the tester was adjusted to an appropriate angle. After the specimen was fractured, the failure load can be read on the scaleplate. The flexural strength (R_f) was calculated by equation (1).

Figure 1: Flexure tester.

$$R_f = \frac{1.5F_fL}{b^3} \quad (1)$$

where F_f is the load at fracture; L is the span of support (100 mm); and b is the prism width (40 mm). The average of three specimens was reported as result.

2.3.5 Tensile strength

Three 305 mm × 76 mm × 20 mm specimens for each mixture were cast to test uniaxial tensile strength based on JTJ E30-2005 [36]. To avoid over gripping, the specimen was wrapped on both ends by carbon cloth using epoxy resin prior to testing. The displacement during the tensile test was measured by a linear variable differential transformer (LVDT) being installed in the middle of the sample. Curves of stress–strain were plotted by a computer automatically. Tensile strain at 50% peak load was ultimate. The reported tensile strength and ultimate strain were the average of three duplicates.

2.3.6 Fracture properties

The fracture properties of composites were investigated using a three-point bending test. The samples used for the bending experiment were precast notched beams with a dimension of 100 mm × 100 mm × 400 mm. As seen in Figure 2(a), the precast notched beam specimen had support span (S) of 300 mm and initial notch length (a_0) of 40 mm. The notch was cut with a width of 3 ± 1 mm and a length to depth ratio (a_0/h) of 0.4. After the specimens were cured for the designed curing period, an electric saw was used to prepare the notch. Before sawing, the accurate lines should be drawn on the two symmetrical side faces of the specimen. The notch depth was controlled using a triangular rule. The setup of the test was presented in Figure 2(b). One LVDT was mounted at the middle of the specimen to monitor deflection at mid-span. A clip-on gage was set on the notch to measure crack mouth opening displacement (CMOD). The bending tests were performed at a rate of 0.05 mm/min. Meanwhile, load, CMOD, and deflection were measured to calculate fracture parameters. The average of three replicates for each mixture was reported as fracture toughness and fracture energy. In addition, the most typical curve was selected among three replicates as the reported curve.

Based on double-K fracture theory, the critical CMOD (V_c) and the critical crack length (a_c) at a peak load (F_{max}) have a relationship as seen in equation (2) from DL/T5332-2005 [37].

$$a_c = \frac{2}{\pi}(h + h_0)\arctan\left(\frac{tEV_c}{32.6F_{max}} - 0.1135\right)^{1/2} - h_0 \quad (2)$$

where a_c is the critical crack length (m); h is the specimen height (0.1 m); h_0 is the thickness of clip extensometer (0.001 m); t is the specimen width (0.1 m); V_c, is the critical value of CMOD (μm); F_{max}, is the peak load (kN); and E, is the elasticity (GPa) determined by equation (3).

$$E = \frac{1}{tc_i}\left[3.7 + 32.6\tan^2\left(\frac{\pi}{2}\frac{a_0 + h_0}{h + h_0}\right)\right] \quad (3)$$

where a_0 is the initial length of notch (0.04 m) and c_i is the CMOD/load on linear stage (μm/kN).

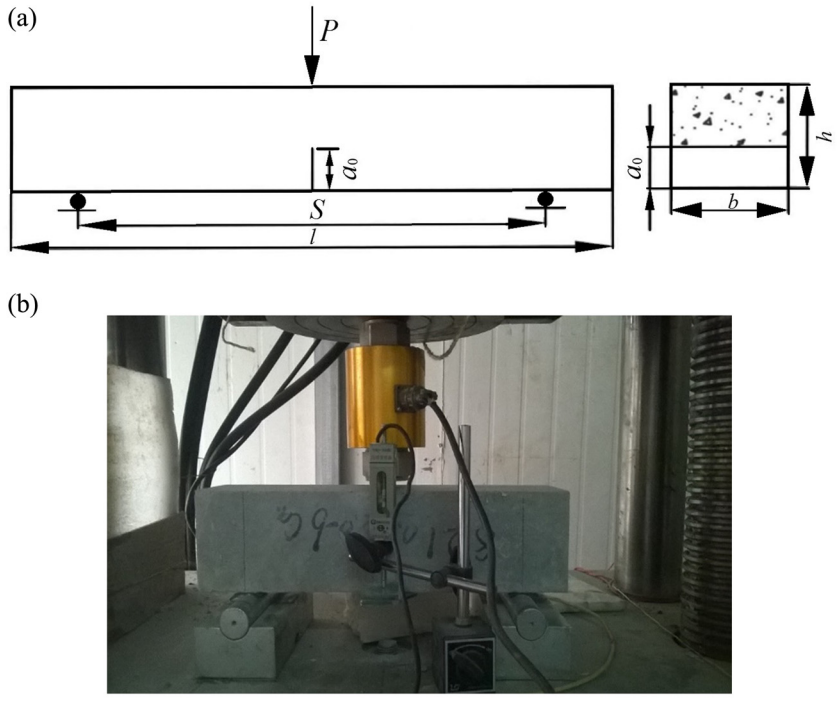

Figure 2: Fracture properties test: (a) dimension of specimen, (b) setup of the bending test.

Fracture toughness (K) has been widely used to assess the fracture properties of concrete [38,39]. During the entire bending test, no crack forms at the first stage where crack propagation is linear elastic. Then, a crack is under elastoplastic propagation until the fracture load [40–42]. The crack initiation load (F_Q) is the load at the breakpoint from linear to nonlinear in the curve of load-CMOD. In accordance with [37], the initiation of toughness was calculated by equations (4) and (5).

$$K_{IC}^{Q} = \frac{1.5 \times \left(F_Q + \frac{mg}{2} \times 10^{-2}\right) \times 10^{-3} \times S \times \sqrt{a_0}}{th^2} \times f(\alpha) \quad (4)$$

$$f(\alpha) = \frac{1.99 - \alpha(1-\alpha)(2.15 - 3.93\alpha + 2.7\alpha^2)}{(1+2\alpha)(1-\alpha)^{3/2}}, \quad \alpha = \frac{a_0}{h} \quad (5)$$

where K_{IC}^{Q} is the initial toughness (MPa m$^{1/2}$); F_Q is the initial crack load (kN); S is the distance of mid-span (0.3 m); m is the weight of mid-span specimen (kg); and g is the gravity acceleration (9.81 m/s^2).

The fracture toughness at peak load is called as unstable fracture toughness which was expressed as equations (6) and (7) according to DL/T5332-2005 [37].

$$K_{IC}^{S} = \frac{1.5\left(F_{max} + \frac{mg}{2} \times 10^{-2}\right) \times 10^{-3} \times S \times \sqrt{a_c}}{th^2} \times f(\alpha) \quad (6)$$

$$f(\alpha) = \frac{1.99 - \alpha(1-\alpha)(2.15 - 3.93\alpha + 2.7\alpha^2)}{(1+2\alpha)(1-\alpha)^{3/2}}, \alpha = \frac{a_c}{h} \quad (7)$$

where K_{IC}^{S} is the unstable fracture toughness (MPa m$^{1/2}$).

The fracture toughness meets:

- If $K < K_{IC}^{Q}$, no crack propagation;
- If $K = K_{IC}^{Q}$, crack starts stable propagation;
- If $K_{IC}^{Q} < K < K_{IC}^{S}$, under stable crack propagation;
- If $K > K_{IC}^{S}$, under unstable crack propagation.

Fracture energy is an indicator of crack resistance and defined as the energy on a unit area in the direction of crack propagation at fracture [43]. It is expressed as equation (8) based on [44].

$$G_F = \frac{W_0}{A} + \frac{mg\delta_0}{A} \quad (8)$$

where W_0 (N m) is the area under the curve of P-CMOD; m (kg) is the m_1 (weight of mid-span specimen) + m_2 (weight of load parts); δ_0 (m) is the deflection in mid-span of fracture; A (m^2) is the net fracture area expressed by equation (9).

$$A = b \times (h - a_0) \quad (9)$$

where h (m) is the height of the sample and b (m) is the width of the sample.

2.3.7 Microstructure

The microstructure of mixtures was investigated using a scanning electron microscope (SEM). The observation areas were represented in the cementitious matrix and fiber fracture of two previously fractured specimens (NS-0.0 and NS-1.5) from the tensile strength test. The observation mode was scattering electron (SE) at 100 × magnification.

3 Results and discussion

3.1 Slump

The results of a slump for the PVA fiber-reinforced mixtures with different NS contents and nanoparticle types are illustrated in Figure 3. It can be seen that the composites with increasing NS content had up to 25% lower flowability. Such effect was due to less water retained on the NS surface caused by more water absorption on its large surface area [45]. Moreover, the gels formed by rapid reactions between dissolved alkalis and NS had a high capacity of water retention [46]. Such a declining effect was also observed for NC, and even greater than NS. Liu et al. found similar results in the effect of NC on flowability [47]. In general, with the same water content, the incorporation of nanoparticles has an adverse influence on the workability of cementitious composites by two mechanisms: (1) the great superficial area of nanoparticles tends to be moist and the trend to assemble can reduce the quantity of free water in the mixture; (2) the tiny nanoparticles will fill into the small holes inside the matrix and improve the connection of the network in the composite [48,49]. Similar findings were reported by Singh et al. indicating that the existence of NS in the matrix enhanced the yield stress and water requirement thus reducing flowability [50].

3.2 Compressive strength

Figure 4 summarizes the results of compressive strength for all composites. It implies that the highest compressive strength among all the fiber-reinforced mixtures was 71.7 MPa at 1.0% NS content. Regardless of NC, 1.0% NS content significantly increased the compressive strength of the cementitious composites by 16%, while higher NS contents hurt the strength.

The initial increase in compressive strength with NS content altering from 0% to 1.0% was associated with the fine NS particles hydrating rapidly as well as providing extra nucleation sites for the growth of CSH gel [51]. Moreover, the NS hydration products filled the void spaces between cementitious grains, fixing the pore water, and decreasing the number of capillary pores [52]. Besides, NS participated in a pozzolanic reaction to produce CSH gels, which promoted the generation of hydration products in turn [51]. The later descending effect with more NS was attributed to the decreased distance between cementitious grains caused by too much NS addition resulting in insufficient cementitious hydration [53]. The 1% nanoparticle addition was reported as optimal by Liu et al. [47] as well. Comparing the compressive strength of the composite containing 2.0% addition of NS and NC, it indicates that the strength of the composites containing NS was higher than that containing NC. This is due to that the NS

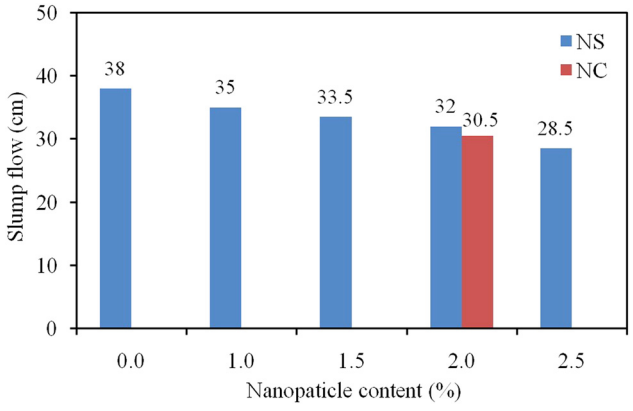

Figure 3: Effects of nanoparticle content and type on slump flow of cementitious composites.

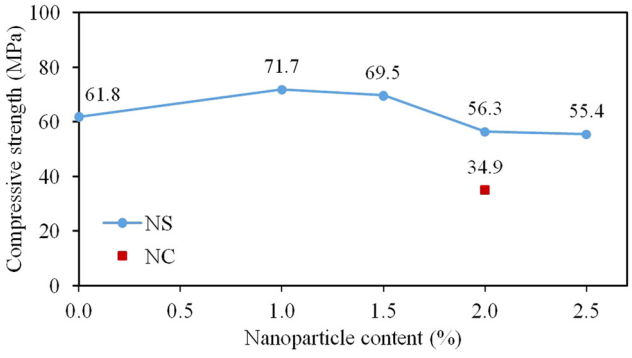

Figure 4: Effects of nanoparticle content and type on compressive strength.

particle has a higher pozzolanic reactivity and hydration which leads to larger amounts of CSH gels, especially in the presence of fly ash [54].

3.3 Flexural strength

The influences of NS content and nanoparticle type in flexural strength are shown in Figure 5. It reveals that with NS content increasing from 0% to 1.5%, the flexural strength considerably increased by up to 12%. This promotion in flexural strength was owing to the filler effect, large surface area, and improvement of pozzolanic activity with NS addition [55]. However, over 1.5% NS addition adversely impacted the flexural strength because excessive NS tends to form abundant ettringite which could lose strength caused by the internal stress [47]. Therefore, the optimal NS content for the flexural strength of fiber-reinforced cementitious composite is 1.5%. Similar to compressive strength, the mixture of NC had lower flexural strength than that of NS for 2.0 content.

3.4 Tensile strength

The relationships between stress and strain during tensile strength tests are presented in Figure 6. Table 6 summarizes tensile strength and ultimate strain of composites. It is noted that the tensile strength was substantially increased with a dosage of NS increasing because of the filler effect of NS which reduced the porosity of composite and the enhanced cement hydration as a consequence of gel formation [56]. About 2.5% NS addition maximally increased the tensile strength by 30.7% which indicates that NS enhancement in

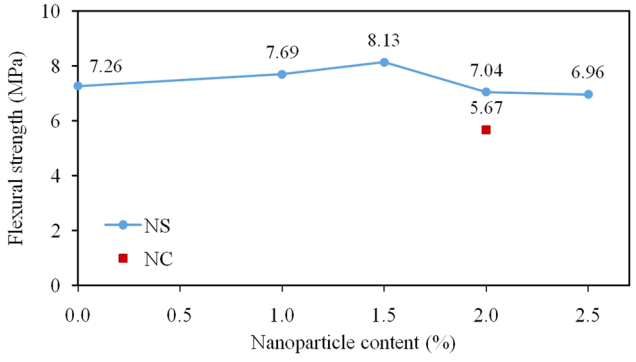

Figure 5: Effects of nanoparticle content and type on flexural strength.

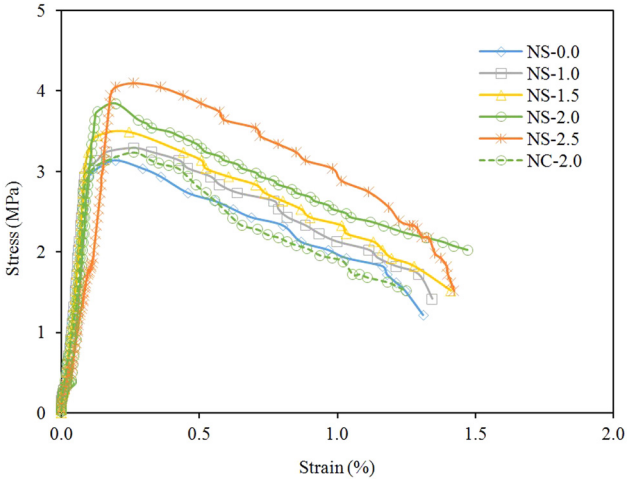

Figure 6: Effect of NS content on tensile stress–strain curve.

tensile strength is more effective than in compression. The interface bond of cementitious composites depends on the bond strength of the interfacial transition zone (ITZ) inside the cementitious composite. With the addition of nanoparticles, the density degree of the ITZ was improved greatly. As a result, the bond between PVA fiber and cementitious matrix was also improved which was confirmed from the microstructure later. However, the ultimate tensile strain was only slightly increased with greater NS (1–2%), and the highest strain was obtained in NS-2.0, which means too much NS could adversely reduce the ductility of PVA fiber-reinforced cementitious composites.

Although NC improved the tensile strength, the strengthening effect was marginal, again mirroring the effects noted above. This is because NC increases the strength only by accelerating the hydration of C_3S [57], while NS participates in the pozzolanic reactions, consuming $Ca(OH)_2$ and producing CSH which becomes more efficient in turn [50,58]. Gaitero et al. also reported that NS could enlarge the mean length of the silicate chain of CSH gel to improve strength [59].

3.5 Fracture properties

Figure 7 illustrates the influence of nanoparticles on the relation curve of load and midspan deflection for all composite mixtures. Based on the area under curves, it can be found that the ductility and toughness greatly increased as NS content increased from 0 to 1.5%, but they declined with more NS addition. This tendency is because NS content within 1.0–1.5% displayed filler effect to reduce porosity in composite matrix by densifying the

Table 6: Tensile properties of mixtures with different NS content

Mix	NS-0.0	NS-1.0	NS-1.5	NS-2.0	NS-2.5	NC-2.0
Tensile strength (MPa)	3.13	3.28	3.49	3.84	4.09	3.24
Ultimate strain (%)	1.31	1.34	1.41	1.47	1.42	1.25

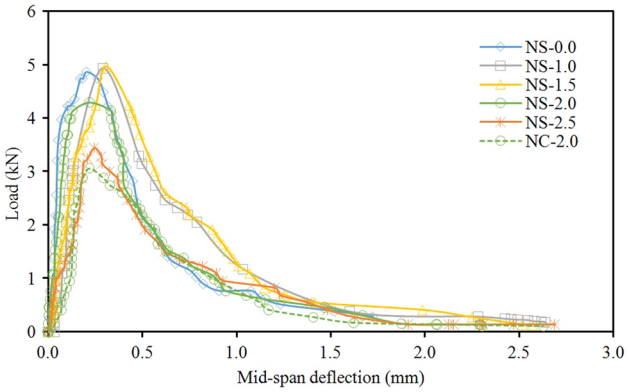

Figure 7: Effect of nanoparticles on the relation curve of load and midspan deflection.

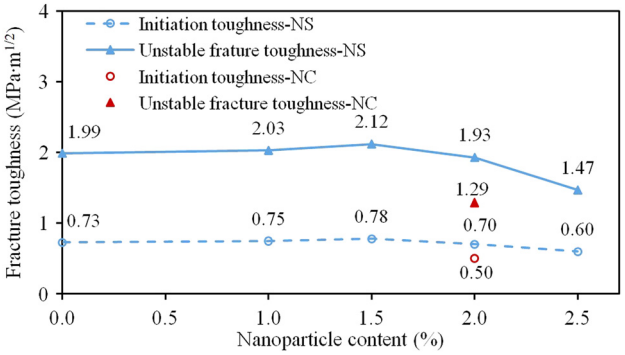

Figure 8: Effects of nanoparticle content and type on fracture toughness.

microstructure and the ITZ [60], while too large content of NS was tendentious to self-desiccation, which leads to microcracks in composites [58].

The effects of nanoparticle content and type on fracture toughness of the composites are presented in Figure 8. As is shown, both the initial toughness and unstable fracture toughness slightly increased as NS content varying from 0% to 1.5%, while they reduced when NS content was higher than 1.5%. This phenomenon means the effect of moderate NS addition was marginal on fracture toughness. However, the excessive addition of NS (>1.5%) could weaken the fracture toughness of the composites. Similar findings were obtained on the mixtures with NC.

Figure 9 shows the fracture energy results. The trend of fracture energy is coincident with that of fracture toughness,

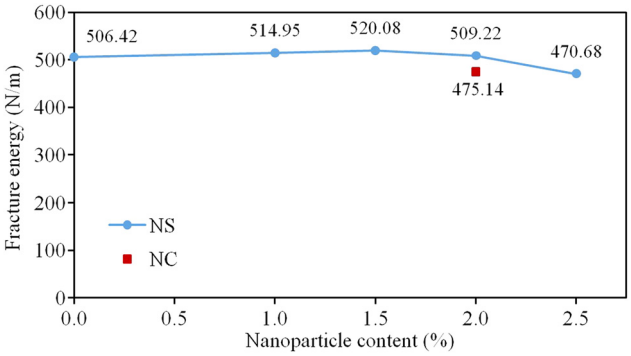

Figure 9: Effects of nanoparticle content and type on fracture energy.

i.e., the higher fracture energy, the larger fracture toughness. This is related to fact that the bonding strength between the PVA fiber and cementitious matrix was enhanced, therefore increasing fracture energy and toughness [61]. However, with excess NS, the fracture energy decreased because of non-uniform NS distribution resulting in agglomeration of NS which increased porosity and weakened the engineering performance of the composites [62]. The fracture indices are presented in Table 7. As can be seen from the table, the fracture energy well explained the effect of NS on a_c and F_{max}. The optimum NS content was 1.5%.

3.6 Fracture properties

SEM images were used to evaluate the influence of NS in the engineering properties of the fiber-reinforced composites.

Table 7: Summary of fracture parameters

Mix	a_c mm	F_{max} N	K_{IC}^{Q} MPa m$^{1/2}$	K_{IC}^{S} MPa m$^{1/2}$	G_F N/m
NS-0.0	66.07	4,872	0.73	1.99	506.42
NS-1.0	68.83	4,934	0.75	2.03	514.95
NS-1.5	69.57	4,973	0.78	2.12	520.08
NS-2.0	63.15	4,228	0.70	1.93	509.22
NS-2.5	61.94	3,452	0.60	1.47	470.68
NC-2.0	61.65	3,059	0.50	1.29	475.14

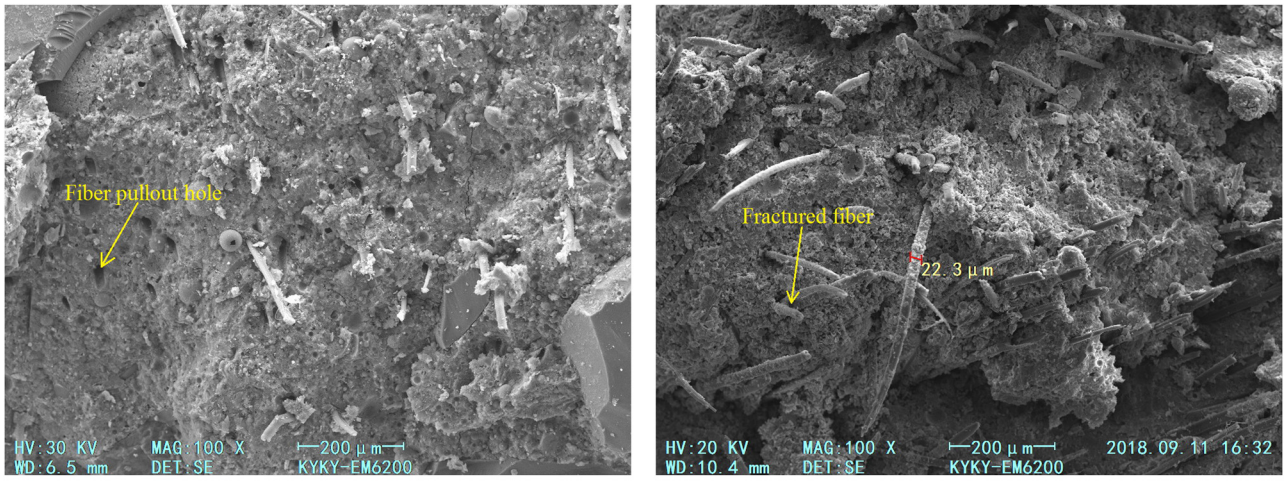

(a) (b)

Figure 10: Microstructures of cementitious composites: (a) NS-0.0, (b) NS-1.5.

The aim was to observe the effect of NS on the failure mode of cementitious composites reinforced with PVA fibers. The microstructures of NS-0.0 and NS-1.5 mixtures at 100× magnification are shown in Figure 10. It can be seen that the microstructure was denser in NS-1.5 than in NS-0.0 specimens. As discussed, the improved density from the filler effect of NS and the promoted cement hydration were the main contributions to the engineering properties of composites with NS addition.

A previous study implies that large amounts of PVA fibers in the cementitious composite substantially enhanced the tensile strength [63]. Conversely, the failure mode of NS-0.0 specimens was predominantly pullout related. The moderate NS addition in PVA fiber-reinforced cementitious composites could significantly increase the bonding strength between the fiber and composite matrix. These findings are consistent with the results found in [61].

4 Conclusions

This paper investigated the effects of NS contents and nanoparticle types on the slump and engineering properties of PVA fiber-reinforced cementitious composites. Based on the test results, conclusions were drawn as follows:

- (1) The addition of nanoparticles decreased the workability of fresh cementitious composites reinforced with PVA fibers. The composites with increasing NS content had up to 25% lower flowability. Higher NS content deceased more workability and NC reduced more workability than NS for the composites.
- (2) There was initial increase and later decrease in compressive and flexural strengths as NS content alters from 0% to 2.5%, while continuous increase was found in tensile strength. 0–1.5% NS addition was optimal to enhance compressive and flexural strengths of composites reinforced with PVA fibers, and 2.5% NS was the best for tensile strength. The composite containing NC exhibited lower strengths than the composite containing same content of NS.
- (3) The fracture energy and initial and unstable fracture toughness slightly increased with NS content varying from 0% to 1.5%, while they reduced when NS content was higher than 1.5%. The composite containing NC had lower ductility and toughness than the composite containing the same content of NS. The effects of NS and NC on the fracture properties were limited.
- (4) NS incorporation of 1.5% decreased porosity and densified the cementitious matrix. It also increased the bonding strength between the fiber and composite matrix. Consequently, most PVA fibers were fractured instead of pull-out during tension by adding NS.

Acknowledgments: The authors would like to acknowledge the financial support received from National Natural Science Foundation of China (Grant No. 51678534), Program for Innovative Research Team (in Science and Technology) in University of Henan Province of China (Grant No. 20IRTSTHN009), CRSRI Open Research Program (Grant No. CKWV2018477/KY), and Open Projects Funds of Dike Safety and Disaster Prevention Engineering Technology Research Center of Chinese Ministry of Water Resources (Grant no. 2018006).

Conflict of interest: The authors declare no conflict of interest regarding the publication of this paper.

References

[1] Huang B, Li Q, Xu S, Zhou B. Tensile fatigue behavior of fiber-reinforced cementitious material with high ductility: experimental study and novel P–S–N model. Constr Build Mater. 2018;178:349–59.

[2] Zhao HT, Jiang KD, Yang R, Tang YM, Liu JP. Experimental and theoretical analysis on coupled effect of hydration, temperature and humidity in early-age cement-based materials. Int J Heat Mass Tran. 2020;146:118784.

[3] Niu H, Wu W, Xing Y, Zhao Y. Effects of the process of polyvinyl alcohol (PVA) fiber bridging cracks and fiber distribution on the bending properties of cementitious composites. J Build Mater. 2016;19:352–8.

[4] Zhang P, Ling YF, Wang J, Shi Y. Bending resistance of PVA fiber reinforced cementitious composites containing nano-SiO_2. Nanotechnol Rev. 2019;8:690–8.

[5] Zhang P, Li QF, Wang J, Shi Y, Ling YF. Effect of PVA fiber on durability of cementitious composite containing nano-SiO_2. Nanotechnol Rev. 2019;8:116–27.

[6] Li QH, Sun CJ, Xu SL. Thermal and mechanical properties of ultrahigh toughness cementitious composite with hybrid PVA and steel fibers at elevated temperatures. Compos Part B. 2019;176:107201.

[7] Yu K, Wang Y, Yu J, Xu S. A strain-hardening cementitious composites with the tensile capacity up to 8%. Constr, Build, Mater. 2017;137:410–9.

[8] Cadoni E, Meda A, Plizzari GA. Tensile behaviour of FRC under high strain-rate. Mater Struct. 2009;42:1283–94.

[9] Haskett M, Mohamed SM, Oehlers D, Guest G, Pritchard T, Sedav V, et al. Deflection of GFRP and PVA fibre reinforced concrete beams, In: Proceedings of the 6th International Conference on FRP Composites in Civil Engineering (CICE2012), Rome, Italy, 2012, p. 13–5.

[10] Ling Y, Wang K, Li W, Shi G, Lu P. Effect of slag on the mechanical properties and bond strength of fly ash based engineered geopolymer composites. Compos Part B. 2019;164:747–57.

[11] Ma H, Qian S, Zhang Z, Lin Z, Li VC. Tailoring engineered cementitious composites with local ingredients. Constr Build Mater. 2015;101:584–95.

[12] Li H, Xu S, Leung CKY. Tensile and flexural properties of ultrahigh toughness cementitious composite. J Wuhan Univ Technol Mater Sci Ed. 2009;24:677–83.

[13] Atahan HN, Pekmezci BY, Tuncel EY. Behavior of PVA fiber-reinforced cementitious composites under static and impact flexural effects. J Mater Civ Eng. 2013;25:1438–45.

[14] Ekaputri JJ, Limantono H, Triwulan T, Susanto T, Abdullah MMAB. Effect of PVA fiber in increasing mechanical strength on paste containing glass powder. Key Eng Mater. 2016;673:83–93.

[15] Topic J, Proseka Z, Indrova K, Plachy T, Nezerka V, Kopecky L, et al. Effect of PVA modification on the properties of cement composites. Acta Polytech. 2015;55:64–75.

[16] Bastos G, Patino-Barbeito F, Patino-Cambeiro F, Armesto J. Nano-inclusions applied in cement-matrix composites: a review. Materials. 2016;9:1015.

[17] Guo K, Miao H, Liu L, Zhou JH, Liu M. Effect of graphene oxide on chloride penetration resistance of recycled concrete. Nanotechnol Rev. 2019;8:681–9.

[18] Gonzalez M, Tighe S, Hui K, Rahman S, Oliveira Lima A. Evaluation of freeze/thaw and scaling response of nano concrete for Portland cement concrete (PCC) pavements. Constr Build Mater. 2016;120:465–72.

[19] Zhang L, Ma N, Wang Y, Han B, Cui X, Yu X, et al. Study on the reinforcing mechanisms of nanosilica to cement-based materials with theoretical calculation and experimental evidence. J Compos Mater. 2016;50:4135–46.

[20] Gesoglu M, Güneyisi E, Asaad DS, Muhyaddin GF. Properties of low binder ultra-high performance cementitious composites: comparison of nanosilica and microsilica. Constr Build Mater. 2016;102:706–13.

[21] Givi AN, Rashid SA, Aziz FNA, Salleh MAM. Experimental investigation of the size effects of SiO_2 nano-particles on the mechanical properties of binary blended concrete. Compos Part B. 2010;41:673–7.

[22] Li Z, Wang H, He S, Lu Y, Wang M. Investigations on the preparation and mechanical properties of the nano-alumina reinforced cement composite. Mater Lett. 2006;60:356–9.

[23] He K, Chen Y, Xie WT. Test on axial compression performance of nano-silica concrete-filled angle steel reinforced GFRP tubular column. Nanotechnol Rev. 2019;8:523–38.

[24] Zhang P, Zheng YX, Wang KJ, Zhang KX. Combined influence of nano-$CaCO_3$ and polyvinyl alcohol fibers on fresh and mechanical performance of concrete incorporating fly ash. Struct Concr, Online. 2019.

[25] Lin QJ, Chen Y, Liu C. Mechanical properties of circular nano-silica concrete filled stainless steel tube stub columns after being exposed to freezing and thawing. Nanotechnol Rev. 2019;8:600–18.

[26] Zhuang CL, Chen Y. The effect of nano-SiO_2 on concrete properties: a review. Nanotechnol Rev. 2019;8:562–72.

[27] GB 175-2007, Common Portland cement, Beijing: China Standards Press, 2007 (in Chinese).

[28] GB/T 1596-2017, Fly ash used for cement and concrete, Beijing: China Standards Press, 2017 (in Chinese).

[29] Yew MK, Mahmud HB, Ang BC, Yew MC. Effects of low volume fraction of polyvinyl alcohol fibers on the mechanical properties of oil palm shell lightweight concrete. Adv Mater Sci Eng. 2015;2015:425236.

[30] ASTM C305, Standard practice for mechanical mixing of hydraulic cement pastes and mortars of plastic consistency, ASTM International, PA, 2014.

[31] Kim SW, Yun HD. Flexural behaviour of reinforced concrete beams strengthened with a composite reinforcement layer: BFRP grid and ECC. Constr Build Mater. 2016;115:424–37.

[32] Felekoglu B, Tosun-Felekoglu K, Ranade R, Zhang Q, Li VC. Influence of matrix flowability, fiber mixing procedure, and curing conditions on the mechanical performance of HTPP-ECC. Compos Part B. 2014;60:359–70.

[33] Wu C, Li VC. Thermal-mechanical behaviors of CFRP-ECC hybrid under elevated temperatures. Compos Part B. 2017;110:255–66.

[34] ASTM C1611, Standard test method for slump flow of self-consolidating concrete, ASTM International, PA, 2018.
[35] JGJ/T70-90, Standard for test method of performance on building mortar, Beijing: Architecture & Building Press, 2009 (in Chinese).
[36] JTJ E30-2005, Test methods of cement and concrete for highway engineering, Beijing: China Communications Press, 2005 (in Chinese).
[37] DL/T 5332-2005, Norm for fracture test of hydraulic concrete, Electric Power Industry Standard, 2005 (in Chinese).
[38] Golewski GL. Green concrete composite incorporating fly ash with high strength and fracture toughness. J Clean Prod. 2018;172:218–26.
[39] Golewski GL. Effect of curing time on the fracture toughness of fly ash concrete composites. Compos Struct. 2018;185:105–12.
[40] Guan J, Hu X, Yao X, Wang Q, Li Q, Wu Z. Fracture of 0.1 and 2 m long mortar beams under three-point-bendiing. Mater Design. 2017;133:363–75.
[41] Guan J, Yuan P, Hu X, Qing L, Yao X. Statistical analysis of concrete fracture using normal distribution pertinent to maximum aggregate size. Theor Appl Fract Mec. 2019;101:236–53.
[42] Guan J, Li C, Wang J, Qing L, Song Z, Liu Z. Determination of fracture parameter and prediction of structural fracture using various concrete specimen types. Theor Appl Fract Mec. 2019;100:114–27.
[43] Aydin AC. Self compactability of high volume hybrid fiber reinforced concrete. Constr Build Mater. 2007;21:1149–54.
[44] Cao P, Feng DC, Zhou CJ, Zuo WX. Study on fracture behavior of polypropylene fiber reinforced concrete with bending beam test and digital speckle method. Comput Concrete. 2014;14:527–46.
[45] Li P. A study on pavement performance of cement concrete with nano particles, Master thesis, Chinese:Chang'an University;2010.
[46] Berra M, Carassiti F, Mangialardi T, Paolini AE, Sebastiani M. Effects of nanosilica addition on workability and compressive strength of Portland cement pastes. Constr Build Mater. 2012;35:666–75.
[47] Liu X, Chen L, Liu A, Wang X. Effect of nano-$CaCO_3$ on properties of cement paste. Energy Procedia. 2012;16:991–6.
[48] Vance K, Kumar A, Sant G, Neithalath N. The rheological properties of ternary binders containing Portland cement, limestone, and metakaolin or fly ash. Cement Concrete Res. 2013;52:196–207.
[49] Ferron RD, Shah S, Fuente E, Negro C. Aggregation and breakage kinetics of fresh cement paste. Cement Concrete Res. 2013;50:1–10.
[50] Singh LP, Karade SR, Bhattacharyya SK, Yousuf MM, Ahalawat S. Beneficial role of nanosilica in cement based materials – a review. Constr Build Mater. 2013;47:1069–77.
[51] Thomas JJ, Jennings HM, Chen JJ. Influence of nucleation seeding on the hydration mechanisms of tricalcium silicate and cement. J Phys Chem C. 2009;113:4327–34.
[52] He X, Shi X. Chloride permeability and microstructure of Portland cement mortars incorporating nanomaterials. Transport Res Rec. 2008;2070:13–21.
[53] Isfahani FT, Redaelli E, Lollini F, Li W, Bertolini L. Effects of nanosilica on Compressive strength anddurability properties of concrete with different water to binder ratios. Adv Mater Sci Eng. 2016;8453567.
[54] Wang X. Effects of nanoparticles on the properties of cement-based materials, Dissertation, Iowa State University;2017.
[55] Atmaca N, Abbas ML, Atmaca A. Effects of nanosilica on the gas permeability, durability and mechanical properties of high-strength lightweight concrete. Constr Build Mater. 2017;147:17–26.
[56] Reches Y. Nanoparticles as concrete additives: review and perspectives. Constr Build Mater. 2018;175:483–95.
[57] Sato T, Beaudoin JJ. Effect of nano-$CaCO_3$ on hydration of cement containing supplementary cementitious materials. Adv Cem Res. 2011;23(1):33–43.
[58] Jo BW, Kim CH, Tae G, Park JB. Characteristics of cement mortar with nano-SiO_2 particles. Constr Build Mater. 2007;21(6):1351–5.
[59] Gaitero JJ, Campillo I, Guerrero A. Reduction of the calcium leaching rate of cement paste by addition of silica nanoparticles. Cement Concrete Res. 2008;38(8):1112–8.
[60] Sanchez F, Sobolev K. Nanotechnology in concrete – a review. Constr Build Mater. 2010;24:2060–71.
[61] Ye Q, Zhang Z, Kong D, Chen R. Influence of nano-SiO_2 addition on properties of hardened cement paste as compared with silica fume. Constr Build Mater. 2007;21:539–45.
[62] Jonbi, Pane I, Hariandja B, Imran I. The Use of nanosilica for improving of concrete compressive strength and durability. Appl Mech Mater. 2012;204–208:4059–62
[63] Wang S, Li VC. Polyvinyl alcohol fiber reinforced engineered cementitious composites: material design and performances. RILEM SARL;2006. p. 65–73.